



## The Influence of the Fundamental Parameters on the Mechanical Behavior of Coarse-Grained Soils

Ghizlane Ardouz <sup>1\*</sup>, Khadija Baba <sup>2</sup>, Latifa El Bouanani <sup>1</sup>, Fatima Ezzahraa Latifi <sup>1</sup>,  
Asmaa Dardouch <sup>2</sup>

<sup>1</sup> 3GIE Laboratory, Mohammed V School of Engineers, Mohammed V University, Rabat, Morocco.

<sup>2</sup> GCE Laboratory, High School of Technology-Salé, Mohammed V University, Rabat, Morocco.

Received 15 April 2022; Revised 05 July 2022; Accepted 14 July 2022; Published 01 August 2022

### Abstract

Coarse-grained soils are a type of soil frequently found in civil engineering projects. The mechanical characterization of these soils is very difficult because of the presence of large-sized elements that disturb or prevent the realization of the tests. However, there is still no rational procedure to characterize coarse soils and determine their mechanical characteristics (cohesion and friction angle) for the calculation of slope stability or structures. The objectives of the research work are to contribute to the improvement of the knowledge of the mechanical behavior of matrix coarse-grained soils and to propose a rational procedure to characterize them. In order to achieve these objectives, it is important to understand the influence of the fundamental parameters related to the mode of reconstitution on the mechanical behavior of the coarse soils: volume fraction, particle size distribution and spread, consolidation level, and the initial state of the matrix. Tests are carried out using the large-sized triaxial testing device in drained conditions. With natural coarse-grained soils, it is very difficult to conduct repeatability tests to validate the results. For this reason, we will study a particular category of coarse-grained soils composed of inclusions (coarse elements) within a fine sandy matrix (matrix coarse-grained soils), using a reference soil composed of a mix of sand and gravel. The results show that for both states of sand compaction ( $I_D=0.4$  and  $I_D=0.8$ ), the shear strength of the soil increases with the increase in the proportion of gravel. This increase is more marked in the case of uniform 8/10 mm gravel. Thus, the size of inclusions has no significant influence on the value of  $q_{max}$ .

**Keywords:** Coarse-Grained Soils, Civil Engineering Projects; Mechanical Behaviour; Matrix; Inclusions.

### 1. Introduction

Coarse soils are a type of soil frequently found in civil engineering projects, and their mechanical characterization still presents a challenge. They are composed of elements of different dimensions (from a few microns to tens of centimeters) and can be of very varied nature (clay, sand, gravel, pebbles, etc.). Matrix coarse-grained soils are a special category of coarse soils. They are composed of inclusions (large elements) of different sizes, surrounded by a fine sandy, silty or clayey matrix. The comprehension of the geo-mechanical behavior of these soils still presents a major problem, because of the presence of large elements that disturb or prevent the realization of the tests.

Coarse soils can be characterized using either in-situ or laboratory tests (Table 1). The in-situ characterization of coarse soils presents many problems related mainly to the expensive testing procedures. Nevertheless, their characterization in the laboratory requires testing of a larger Representative Elemental Volume (REV) of soil [1-3]. During the sampling of these materials, large grains are usually clipped to reduce the volume of soil sampled and returned to the laboratory for the various geotechnical tests. This procedure (clipping + reshuffling) leads to an

\* Corresponding author: [ghizlane.ardouz@mail.com](mailto:ghizlane.ardouz@mail.com)



<http://dx.doi.org/10.28991/CEJ-2022-08-08-012>



© 2022 by the authors. Licensee C.E.J., Tehran, Iran. This article is an open access article distributed under the terms and conditions of the Creative Commons Attribution (CC-BY) license (<http://creativecommons.org/licenses/by/4.0/>).

underestimation of the mechanical characteristics of the material. Therefore, it is very important to be able to characterize the coarse soils in a laboratory with classic-sized equipment, which requires their reconstitution by capping or substituting the large elements.

**Table 1. Limitations of the use of classical reconnaissance tests in situ and in laboratory**

In situ tests: Penetrometer tests or penetrometer or pressuremeter tests or scissometer tests	<ul style="list-style-type: none"> <li>- The driving or ramming operations carried out during the execution of static or dynamic penetrometer tests or scissometer characterization tests are hampered by the presence of large elements (rocks or blocks) in coarse soils.</li> <li>- The dimensions of standard penetrometers and pressometers are too small compared to the size of the coarse soil constituents.</li> </ul>
Laboratory characterization, using standard size testing devices	<ul style="list-style-type: none"> <li>- The large size of the elements contained in these soils makes it difficult to carry out representative tests on standard size specimens.</li> <li>- The diameter of the largest grains is greater than the admissible diameter (<math>d_{\max} &gt; d_{\text{admissible}}</math>)</li> </ul>

Capping consists to remove the large elements of the soil, so the proportion of these elements decreases. Therefore, it is necessary to understand the influence of the volume fraction of inclusions on the behavior of coarse soils [4, 5]. The substitution process consists to replace the larger inclusions with smaller ones, which requires an understanding of the effect of inclusions size and particle distribution on the mechanical behavior of coarse soils [6-8]. Finally, the method of particle size reconstruction by similarity consists to test in a laboratory a soil that is composed of elements whose maximum size is less than or equal to the admissible diameter, and whose granulometric curve is parallel to that of the real soil [7, 8]. However, there is still no rational procedure to characterize coarse soils and determine their mechanical characteristics (cohesion and friction angle) for the calculation of slope stability or structures.

The objectives of the research work are to contribute to the improvement of the knowledge of the mechanical behavior of matrix coarse-grained soils and to propose a rational procedure to characterize them. In order to achieve these objectives, it is important to understand the influence of the fundamental parameters related to the mode of reconstitution on the mechanical characteristics of the coarse soils: volume fraction, particle size distribution and spread, consolidation level, and the initial state of the matrix. In this study, we first present the type of reference soil used and the choice of constituents (matrix and inclusions), and the procedure for manufacturing the samples. Then, we present the experimental results obtained corresponding to the influence of the properties of the inclusions (Volume Fraction:  $f_v$ , size and granulometric spread) on the mechanical behavior for two density indices of the matrix: 0.70 and 0.30. Using the large-sized triaxial testing device, in drained conditions.

Then, the influence of the matrix density state and the isotropic confining stress  $\sigma'_c$  on the results obtained is examined. Finally, from the test results, we estimate the fracture characteristics of the material.

## 2. Materials and Methods

### 2.1. Materials Characterization

Many researchers have used natural coarse soils in laboratory to study their mechanical behavior [9-11], but these materials present difficulties in performing repeatability tests to allow validation of the results obtained. For this reason, we chose to work with a reference soil that allows us to obtain a good repeatability of the tests, and to highlight the influence of the fundamental parameters on the mechanical behavior of this soil. Namely the volume fraction, the size and granulometric spread of the inclusions, the state of compactness of the matrix and the level of consolidation of the specimens.

This reference soil is, composed by a matrix and inclusions (the ratio between the average size of the matrix ( $d_{50,\text{mat}}$ ) and that of the inclusions ( $d_{50,\text{incl}}$ ),  $d_{50,\text{incl}}/d_{50,\text{mat}}$  must be greater than 10 [12, 13] so that the matrix can be considered homogeneous in relation to the inclusions). Also, the inclusions are arranged randomly and are not in contact [13, 14] (Figure 1).

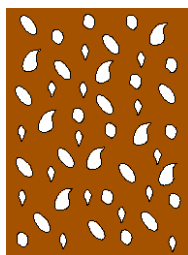


**Figure 1. Representative diagram of a coarse matrix soil**

Figure 2 shows the granulometric curve of the sand used.

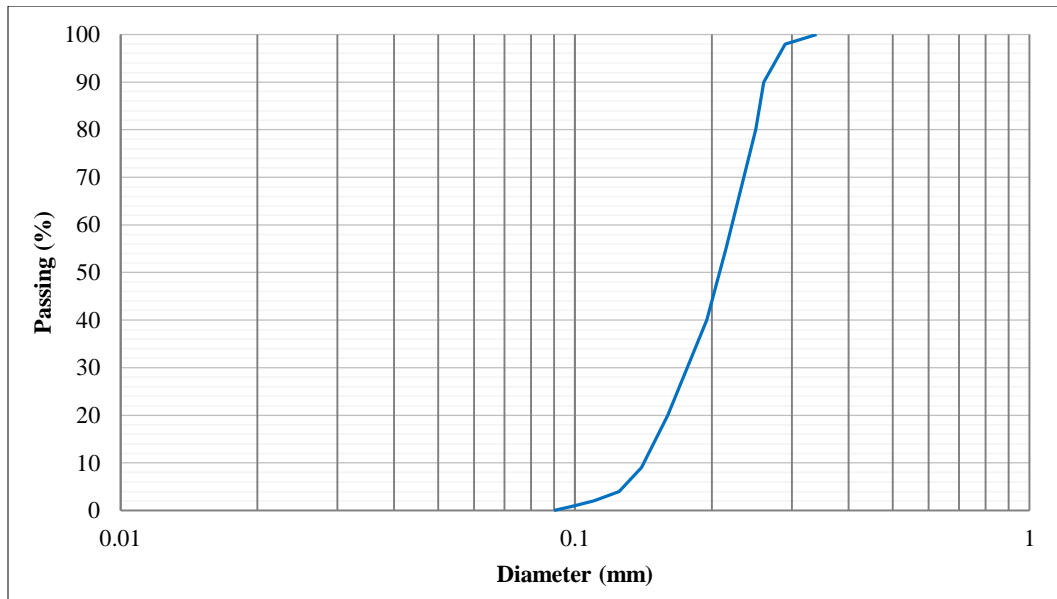


Figure 2. Granulometric spread of the sand used

The physical characteristics of the sand are listed in Table 2.

Table 2. Characteristics of the sand used

D <sub>50</sub>	C <sub>U</sub>	e <sub>min</sub>	e <sub>max</sub>	ρ <sub>s</sub> (g/cm <sup>3</sup> )	ρ <sub>d,min</sub> (g/cm <sup>3</sup> )	ρ <sub>d,max</sub> (g/cm <sup>3</sup> )
0.21	1.52	0.54	0.94	2.65	1.37	1.72

The selected inclusions are natural gravels with density  $\rho_s = 2.65 \text{ g/cm}^3$ , and a maximum diameter of 60 mm (Figure 3).



Figure 3. View of the gravel: 10/20 mm gravel (a) and 4/60 mm gravel (b)

## 2.2. Experimental Procedure

The void ratio of the sand allows us to have its state of compactness:

$$e = e_{\max} - I_D(e_{\max} - e_{\min}) \rightarrow I_D = \frac{e_{\max} - e}{e_{\max} - e_{\min}} \quad (1)$$

Moreover, we have by definition:

$$e = \frac{\rho_{s,sand}}{\rho_{d,sand}} - 1 \text{ so } \rho_{d,sable} = \frac{\rho_{s,sand}}{1+e} \quad (2)$$

where  $\rho_{d,sand}$  is bulk density of the sand matrix.

This allows obtaining the mass of the matrix to be introduced:

$$\rho_{d,sand} = \frac{M_{s,sand}}{V_{sand}} \rightarrow M_{s,sand} = \rho_{d,sand} \times V_{sand} \quad (3)$$

with  $M_{s,sand}$  is Dry mass of the sand.

We define the volume fraction of inclusions noted  $f_v$ , the ratio between the volume of inclusions and the total volume of the specimen. For our study,  $f_v$  varied between 0 and 35%.

$$f_v = \frac{V_G}{V_{Total}} \quad (4)$$

where  $V_G$  is the volume of inclusions and  $V_{Total}$  is the total volume of the specimen.

Since  $f_v$  and  $V_{Total}$  are known, we can deduce the corresponding volume of inclusions:

$$V_G = f_v \times V_{Total} \quad (5)$$

So:

$$M_G = \rho_{s,G} \times V_G \quad (6)$$

with  $M_G$  is mass of inclusions,  $\rho_{s,G}$  is volume mass of the inclusions.

The specimens are made by compacting the material in successive layers of ten layers of soil, each 6 cm thick (Figure 4).

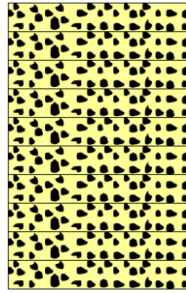


Figure 4. Fabrication of a soil test specimen

### 2.3. Experimental Program

Figure 5, shows the flowchart of the research methodology through which the objectives of this study were achieved. The experimental program consists of 54 tests on 36 different soil mixtures:

- For two matrix compactness states;
- Three states of isotropic consolidation stress:  $\sigma'_c = 50, 100$  and  $400$  kPa;
- A volume fraction  $f_v$  of the inclusions: 0, 12, 20 and 35 %;
- Classes of the inclusions: 8/10 mm, 8/20 mm, 10/20 mm, 30/60 mm and 4/60 mm.

Through the tests performed, the effect of various parameters on the observed behaviors was studied:

- The proportion of inclusions  $f_v$ ;
- The size and granulometric spread of the inclusions;
- The initial compactness state of the sand;
- The level of consolidation applied ( $\sigma'_c$ ).

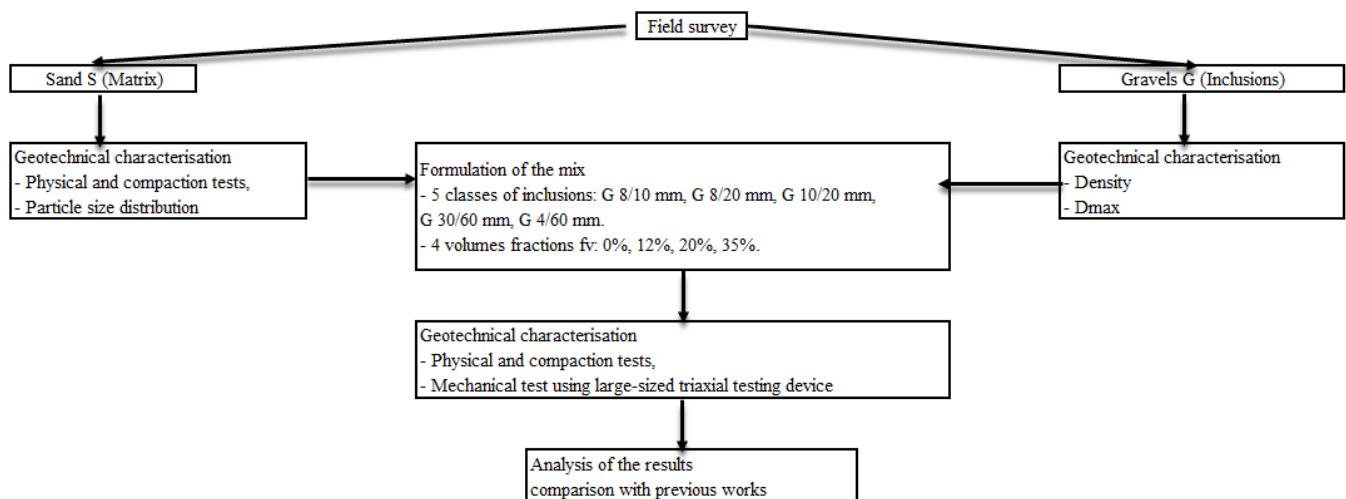
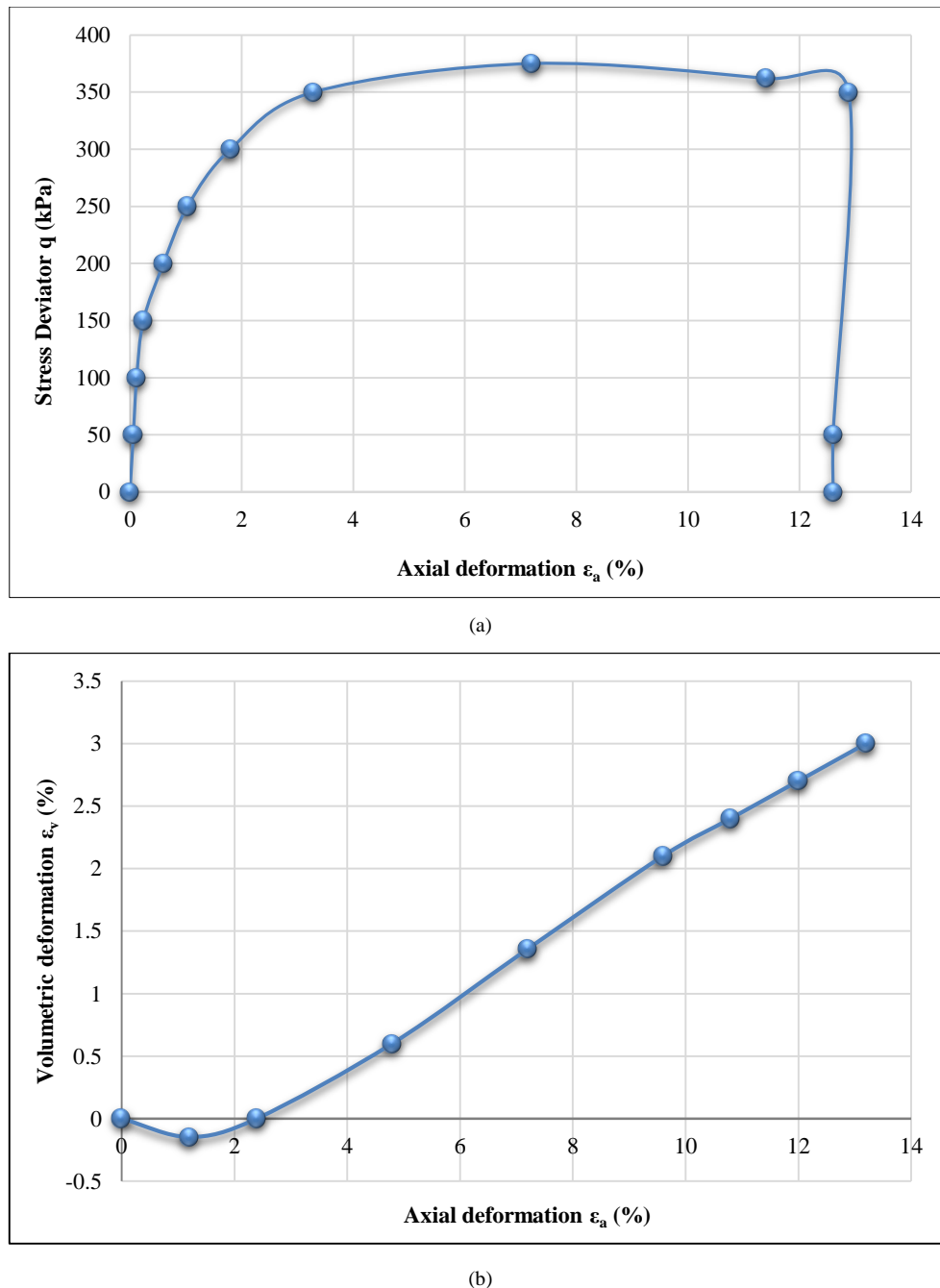


Figure 5. Experimental method

### 3. Typical Test and Repeatability

The Figure 6 presents the results obtained for a typical test on sand without inclusions ( $f_v = 0\%$ ),  $\sigma'_c = 100$  kPa and two  $I_D$  (0.4 and 0.8%).



**Figure 6. The typical test performed on pure sand ( $I_D = 0.8\%$  and  $\sigma'_c = 100$  kPa): (a) shear curve; (b) volumetric deformation curve**

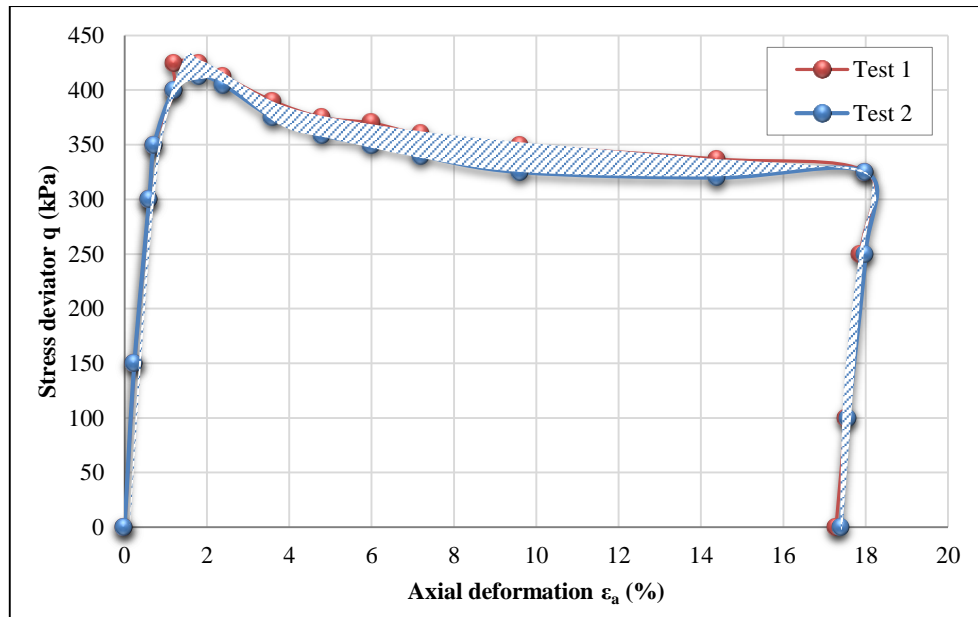
Figure 6-a presents the stress deviator  $q$  as a function of the axial strain  $\epsilon_a$ . It can be seen that the deviator initially increases in a quasi-linear way; this is the elastic phase, followed by the strain-hardening phase corresponding to the failure of the specimen, where  $q$  passes through a peak (here about 376 kPa) for an axial strain about 6%, followed by a softening.

Figure 6-b, represents the volume deformation curve- $\epsilon_v$  as a function of the axial deformation  $\epsilon_a$ . We observe that at the beginning of the loading, the volume of the sample decreases the arrangement of the sand grains. This is the contracting phase (positive volume deformation  $\epsilon_v$ ). Then the sand expands. The point of change in behavior ( $\epsilon_v = 0$ ) corresponds to the characteristic state.

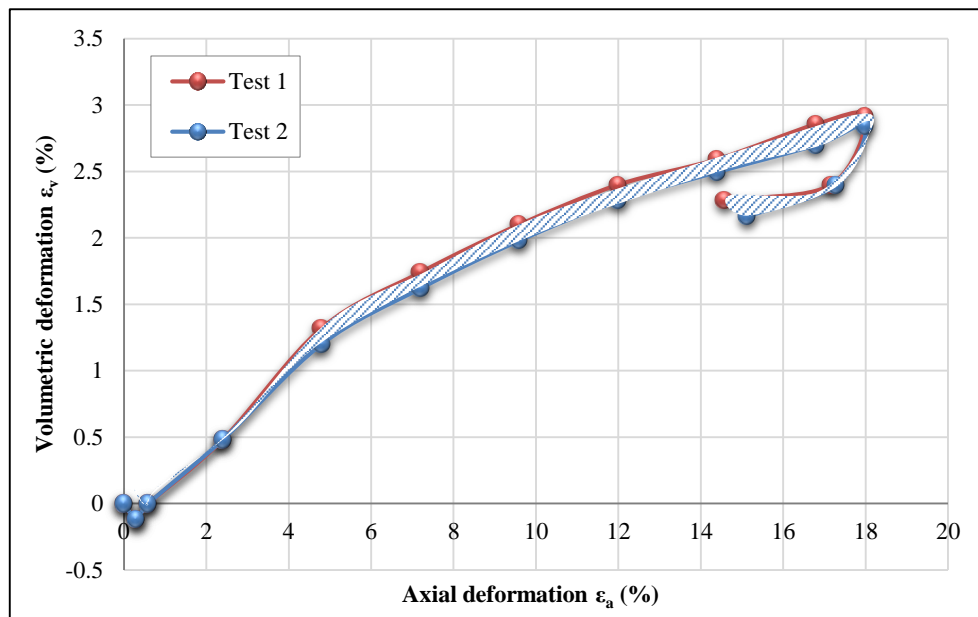
To validate the experimental procedure followed and the results obtained, it was necessary to ensure repeatability

[15, 16], and this, by carrying out two drained tests on specimens composed by sand and 20% gravel 10/20 mm, and two tests on pure sand. Good repeatability is observed for pure sand and mixtures (sand + inclusions).

From these tests (Figures 7 and 8), we define the repeatability spindle (the envelope of the curves corresponding to these tests). This spindle for  $f_v = 20\%$  will be used thereafter and will make it possible to conclude on the influence of the fundamental parameters on the behavior of the studied coarse soils.



(a)



(b)

Figure 7. Repeatability tests on a reference coarse soil ( $I_D=0.8\%$  and  $\sigma'_c=100\text{kPa}$ ): (a) shear curves; (b) volumetric deformation curves

## 4. Influence of the Study Parameters

### 4.1. Influence of the Volume Fraction of the Inclusions $f_v$

The first analysis focused on the effect of the volume fraction. Several tests were performed on specimens composed of sand and 10/20 mm gravel at different volume fractions  $f_v$ . The results are presented as shear curves and volume deformation curves (Figures 9 and 10).

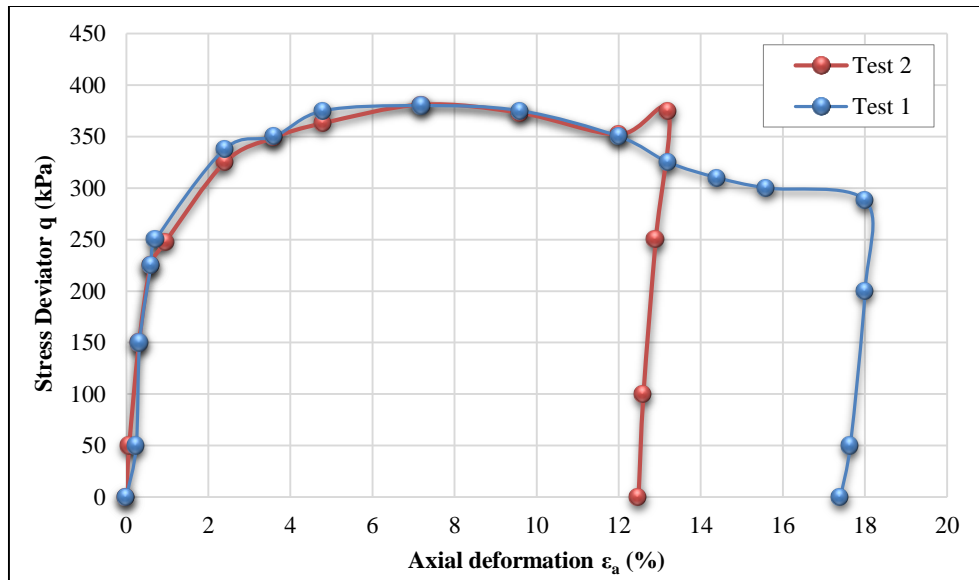


Figure 8. Repeatability tests on pure sand ( $I_D=0.8\%$  and  $\sigma'_c=100\text{kPa}$ )

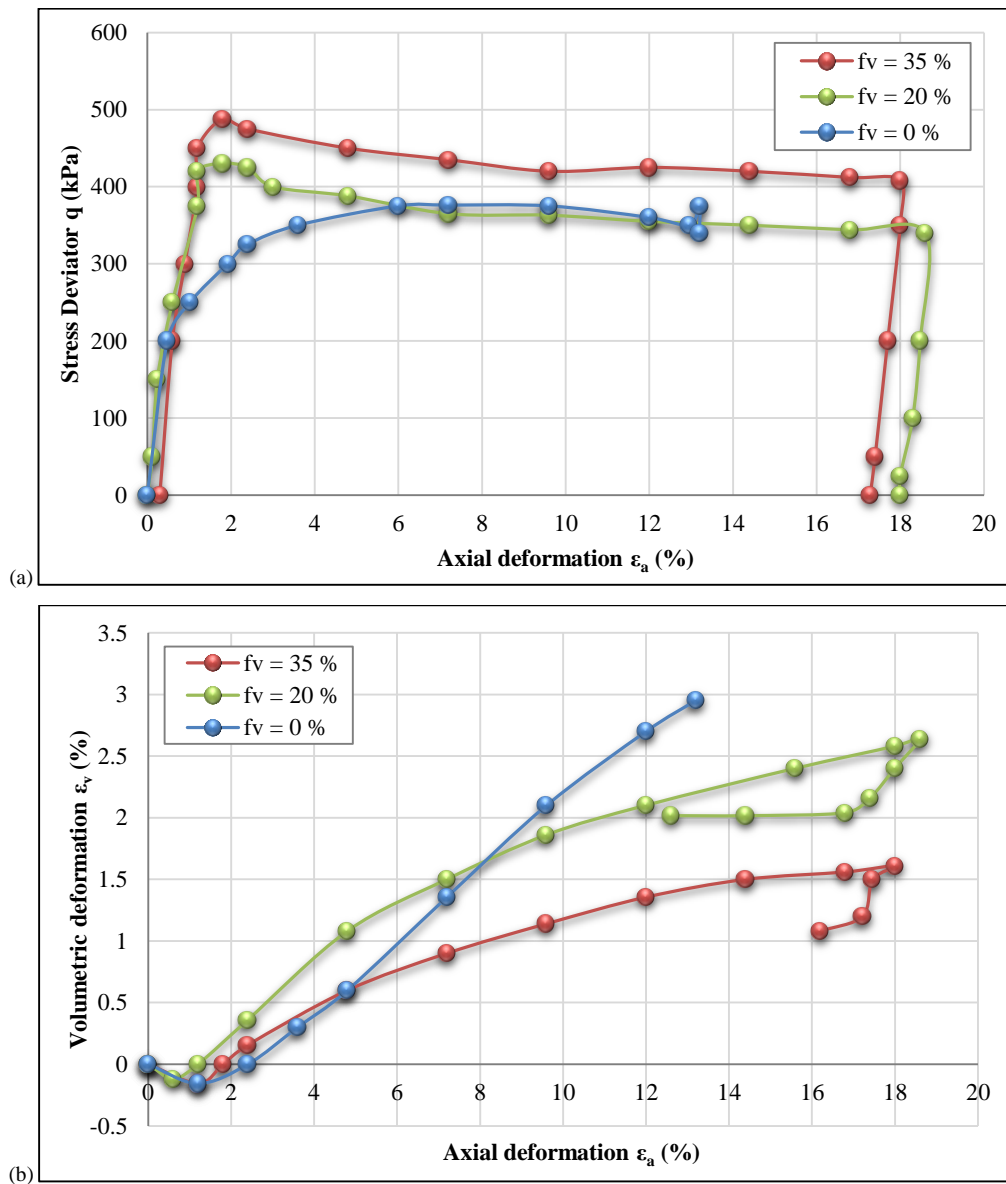
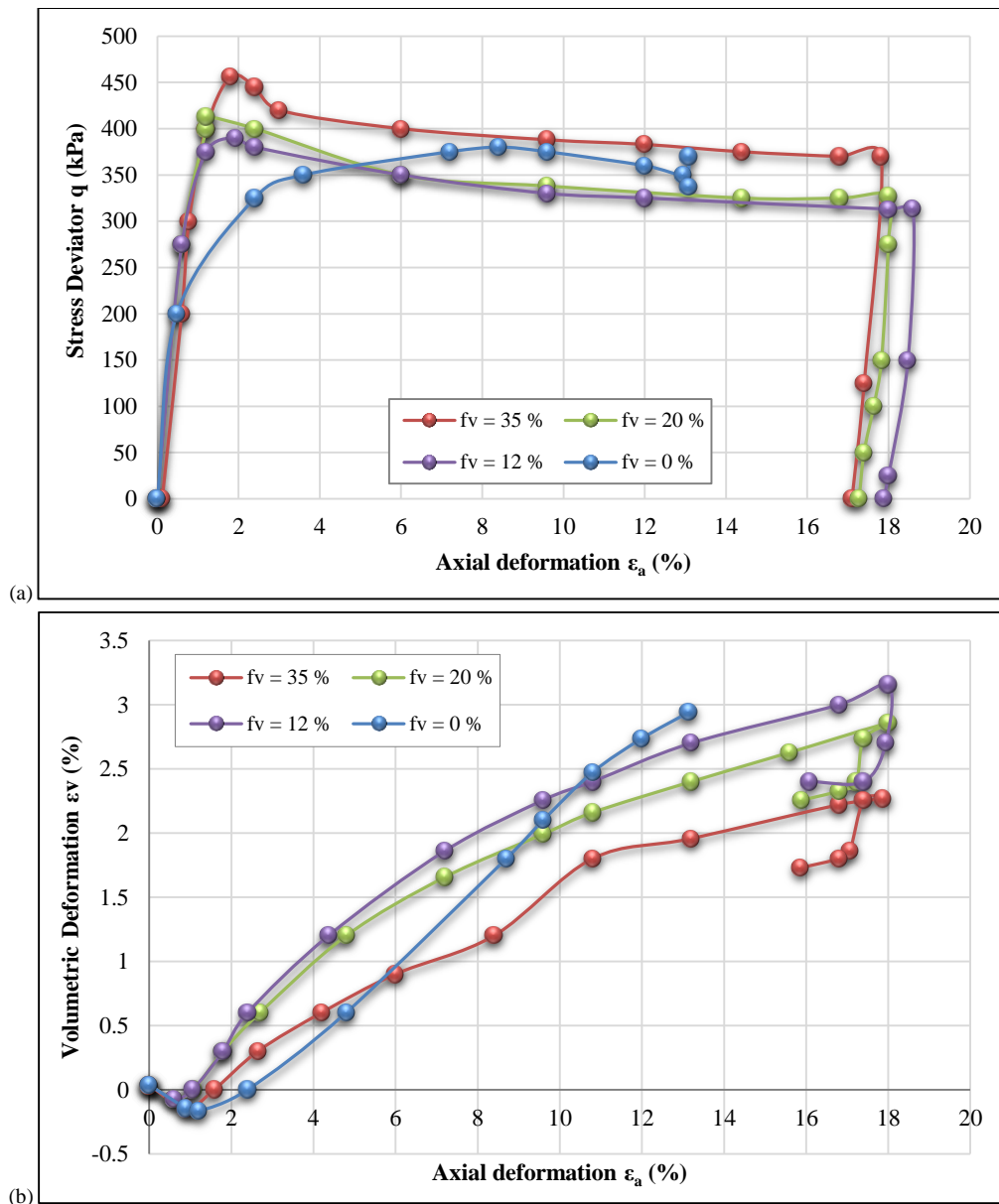
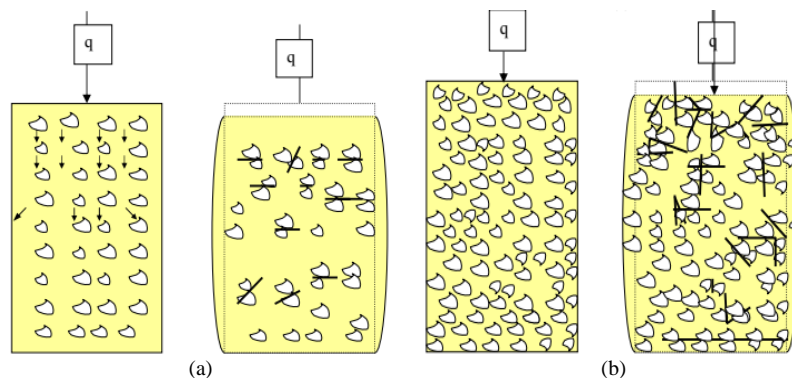


Figure 9. Influence of the volume proportion of gravel  $f_v$ : (a) shear curves; (b) volumetric deformation curves (G 30/60mm,  $I_D=0.8\%$  and  $\sigma'_c=100\text{kPa}$ )



**Figure 10. Influence of the volume proportion of gravel  $f_v$ : (a) shear curves; (b) volumetric deformation curves ( $G_{10/20\text{mm}}$ ,  $I_D=0.8\%$  and  $\sigma'_c=100\text{kPa}$ )**

An increase in the deviator at failure with the proportion of inclusions is observed (Figure 9-a). The softening phase is more significant than the proportion  $f_v$  is high. We also notice a "ductile" behavior for the pure sand with rupture reached for deformation of 8%, to a "fragile" behavior for the sand-gravel mixture with a peak of resistance reached for deformation of 2%. These observations can be explained by the fact that with the increase of  $f_v$ , the contact between gravels becomes more important contributing to the reinforcement of the soil [17-19] (Figure 11). This forms during the test a more shear-resistant surface.



**Figure 11. Grain contact areas during the triaxial test: (a)  $f_v = 12\%$ ; (b)  $f_v = 35\%$**

Regarding the volume deformations (Figure 9-b), the results obtained show that the soil becomes less dilatant by increasing the proportion of inclusions. The same observations for the tests carried out on the mixture of sand with gravel 10/20 mm (Figure 9). The same analysis has been established for soil with gravel G10/20mm and a compactness index  $I_D = 0.4\%$  (Figure 12); from the point of view of volume deformation, we find a mainly contracting behavior.

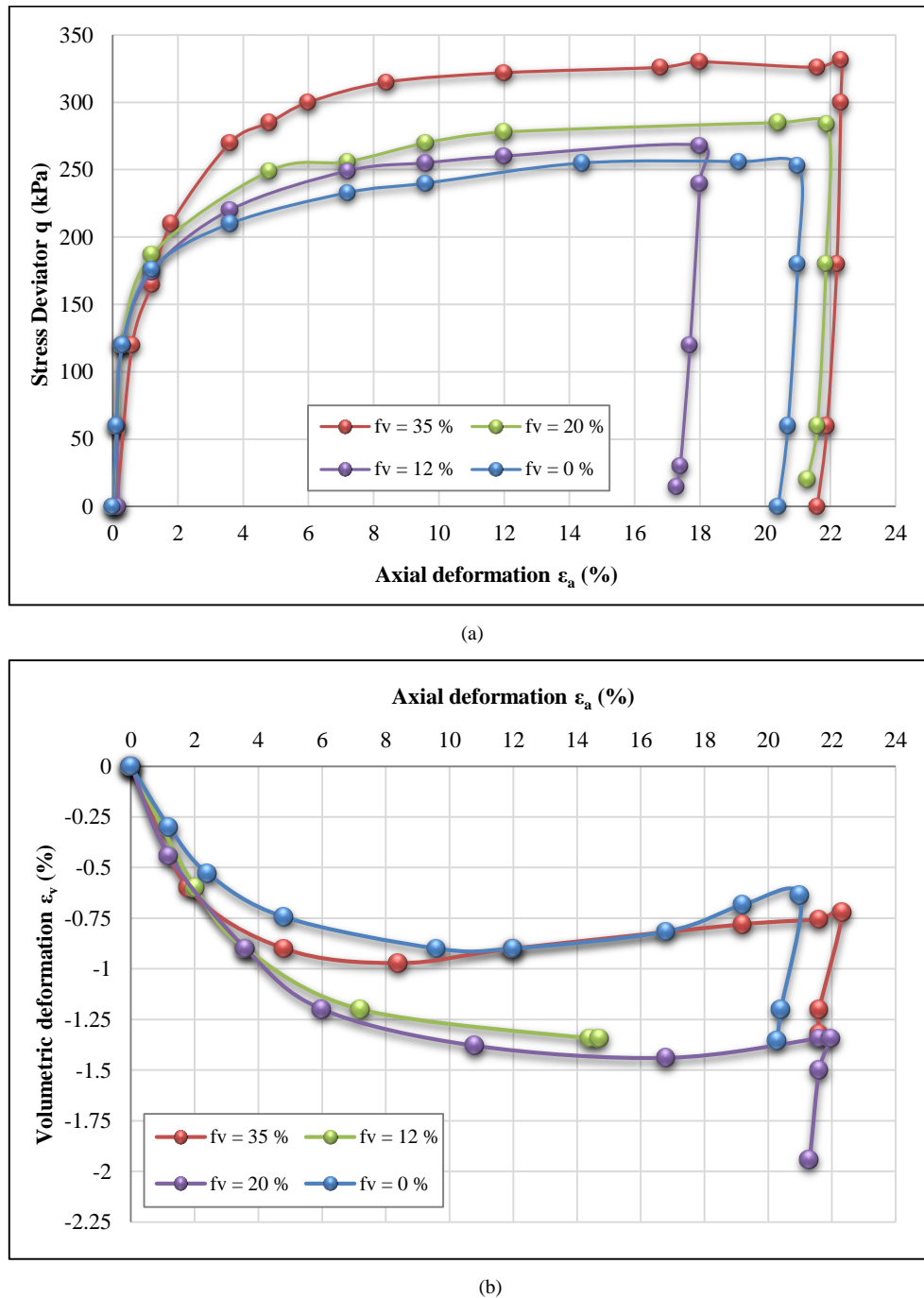


Figure 12. Influence of the volume proportion of gravel  $f_v$ : (a) shear curves; (b) volumetric deformation curves (G 10/20mm,  $I_D = 0.4\%$  and  $\sigma'_c = 100\text{kPa}$ )

#### 4.2. Influence of the Maximum Diameter ( $d_{max}$ ) of the Gravel

To highlight the effect of inclusions size on the shear strength of the coarse soil, we performed several tests by varying the size of the gravel (With two granulometric distributions: 10/20 mm and 30/60 mm, different volume fractions, two compactness indices (0.4% and 0.8%) and for the same initial conditions of  $\sigma'_c$ ). We also traced the repeatability spindle for 20% of the 10/20 mm gravel. Figure 13 shows the results obtained for  $I_D = 0.8\%$  (dense matrix), and Figure 14 shows those for  $I_D = 0.4\%$  (loose matrix).

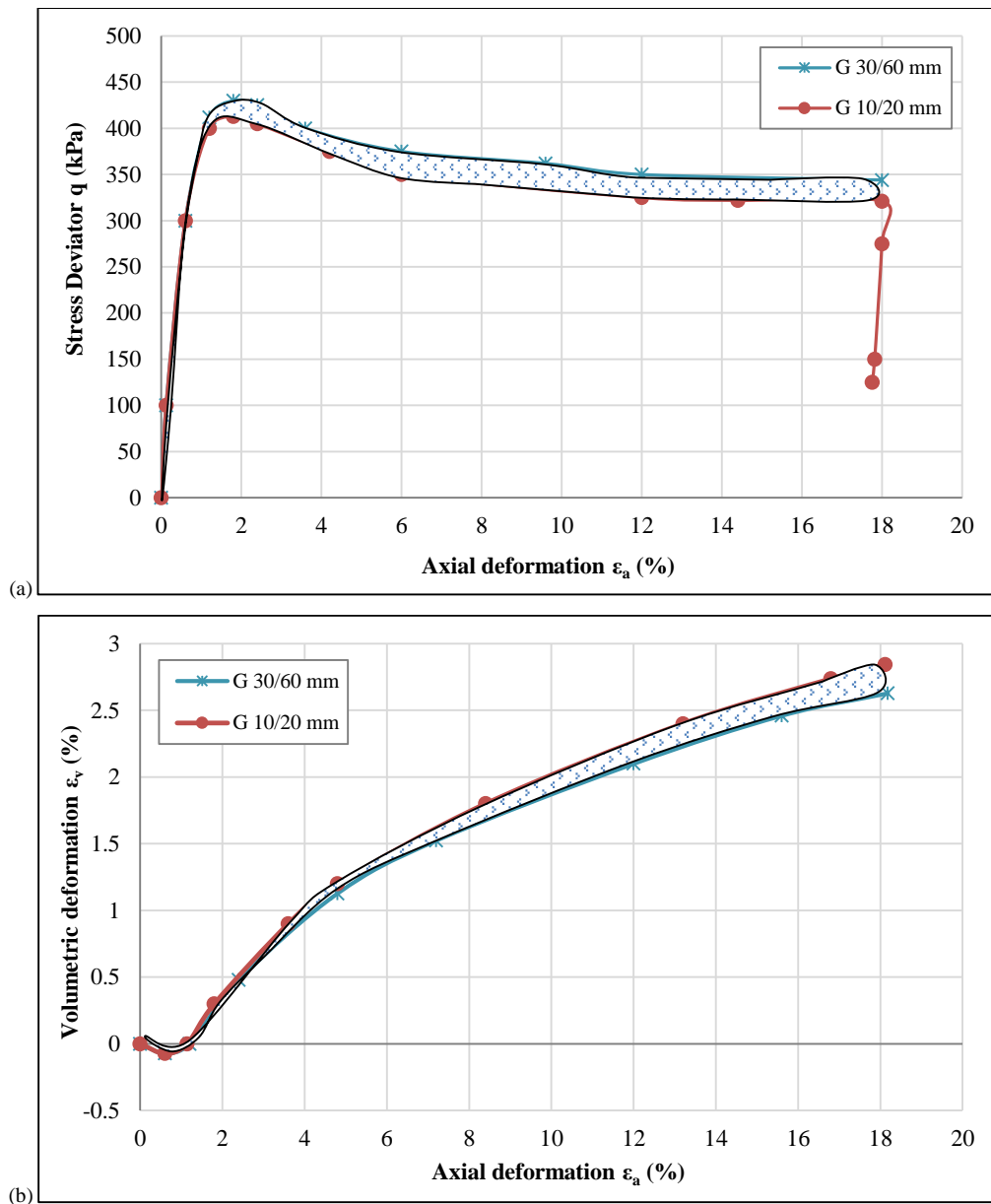
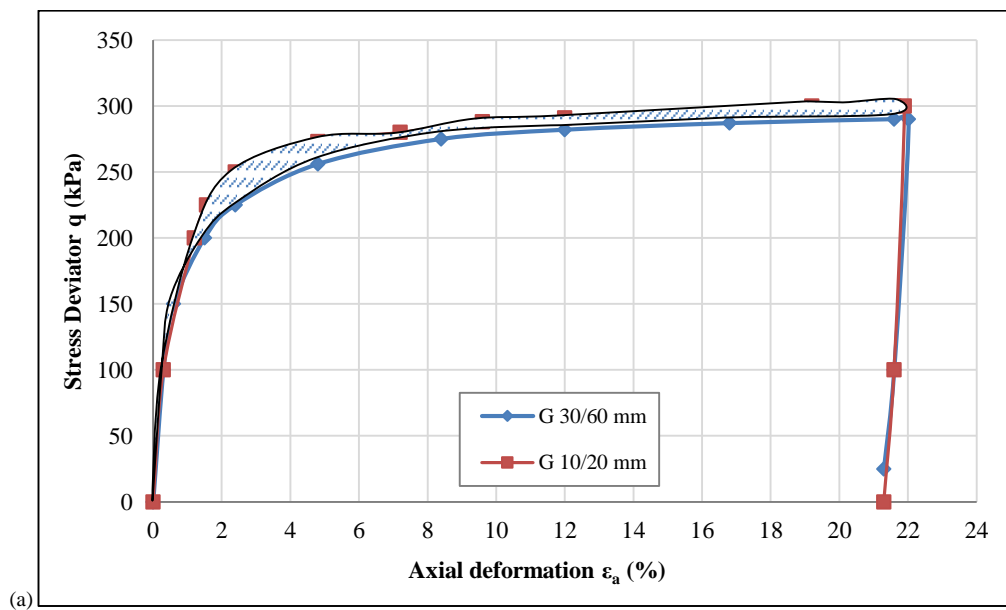


Figure 13. Influence of maximum gravel diameter  $d_{max}$ : (a) shear curves; (b) volumetric deformation curves ( $f_v=20\%$ ,  $I_D=0.8\%$  and  $\sigma'_c=100\text{kPa}$ )



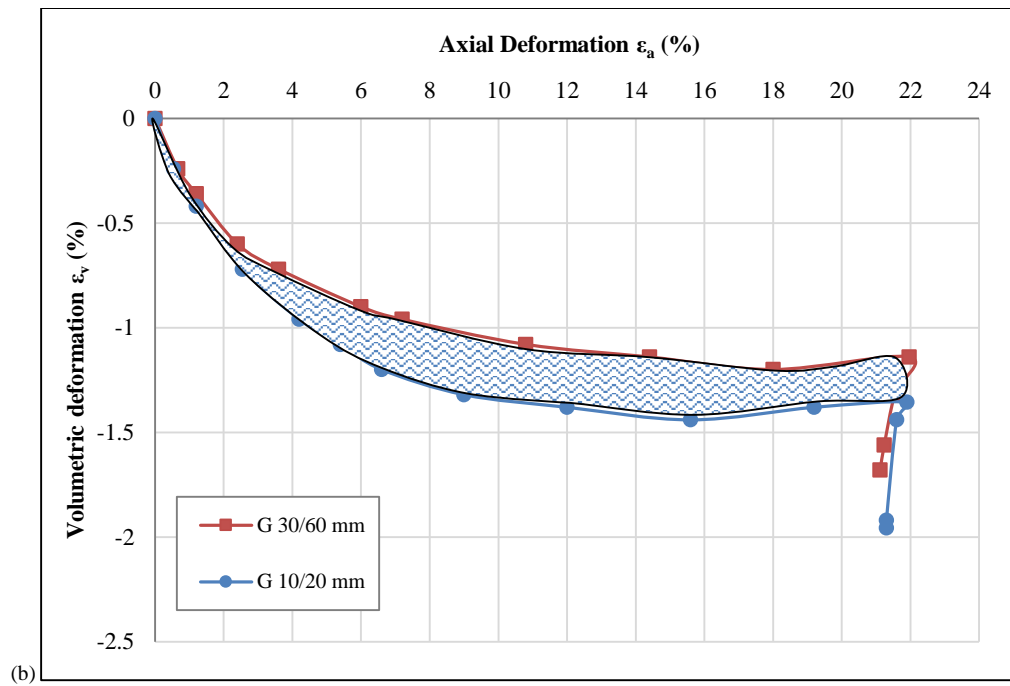


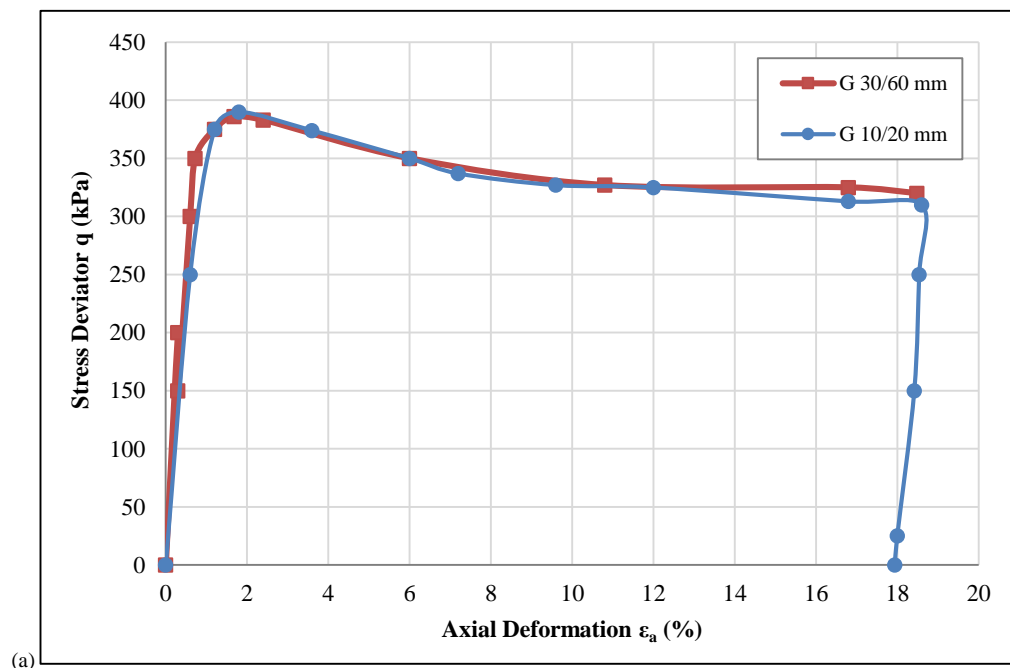
Figure 14. Influence of maximum gravel diameter  $d_{max}$ : (a) shear curves; (b) volumetric deformation curves ( $f_v=20\%$ ,  $I_D=0.4\%$  and  $\sigma'_c=100\text{kPa}$ )

It can be seen from the relatively small differences between the shear curves for the 10/20mm and 30/60mm gravels (Figure 13-a and 14-a) that the size of the inclusions does not have a significant effect on the rupture strength of the soil (the shear curve obtained for the 30/60mm gravel falls within the repeatability range) [20]. On the other hand, concerning the volume deformations (figure 13-b and 14-b), we notice that there is no significant influence of the size of the gravels during the contracting phase. However, in the dilatation phase, it is clear that with the 30/60 mm gravels, the soil is less dilatant.

The same results were demonstrated for volume fractions of 12% and 35% (Figure 15). A slight increase in the deviator at rupture was observed by increasing the volume fraction  $f_v$ . This can be justified by the increase in gravel-gravel contact with increasing size and volume fraction  $f_v$  [21, 22].

#### 4.3. Influence of the Granulometric Spread

Concerning the granulometric spread, we first carried out a series of tests on specimens with 20% and 35% of gravel 10/20 mm, 30/60 mm, 10/60 mm and 4/60 mm with an  $I_D=0.8\%$ . Figures 16 and 17 synthesize the results obtained.



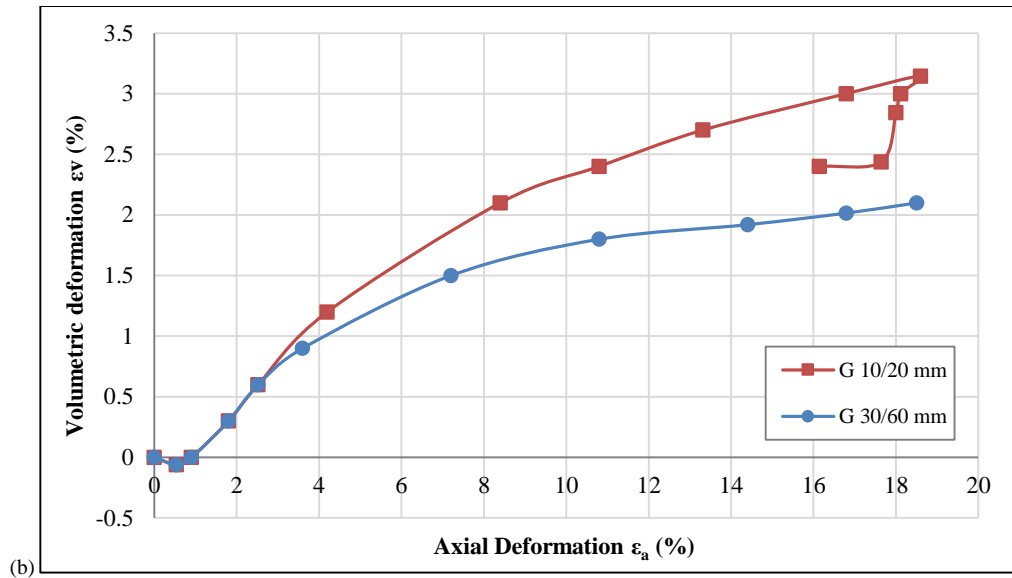


Figure 15. Influence of maximum gravel diameter  $d_{max}$ : (a) shear curves; (b) volumetric deformation curves ( $f_v=12\%$ ,  $I_D=0.8\%$  and  $\sigma'_c=100\text{kPa}$ )

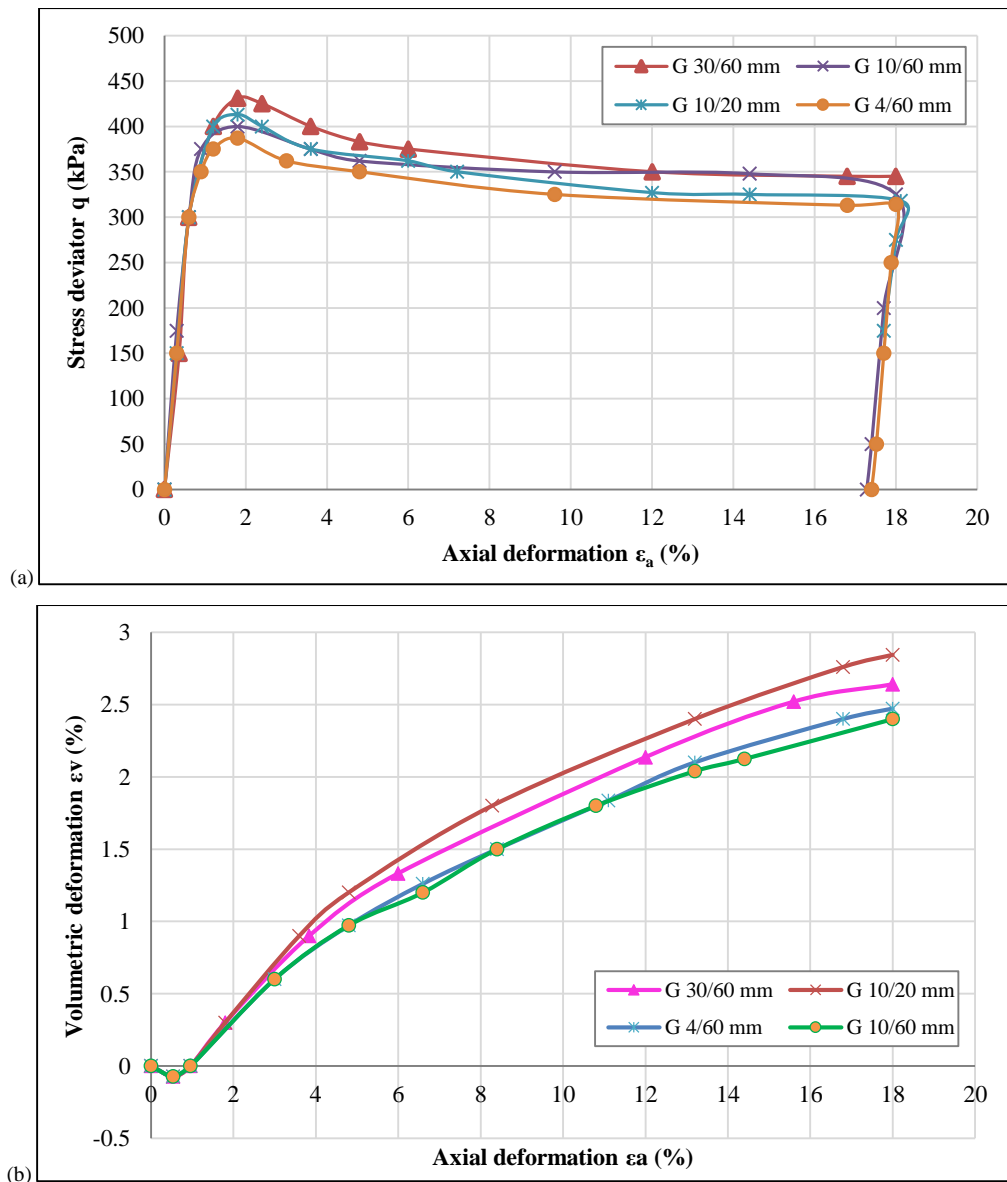


Figure 16. Influence of granulometric spread: (a) shear curves; (b) volumetric deformation curves ( $f_v=20\%$ ,  $I_D=0.8\%$  and  $\sigma'_c=100\text{kPa}$ )

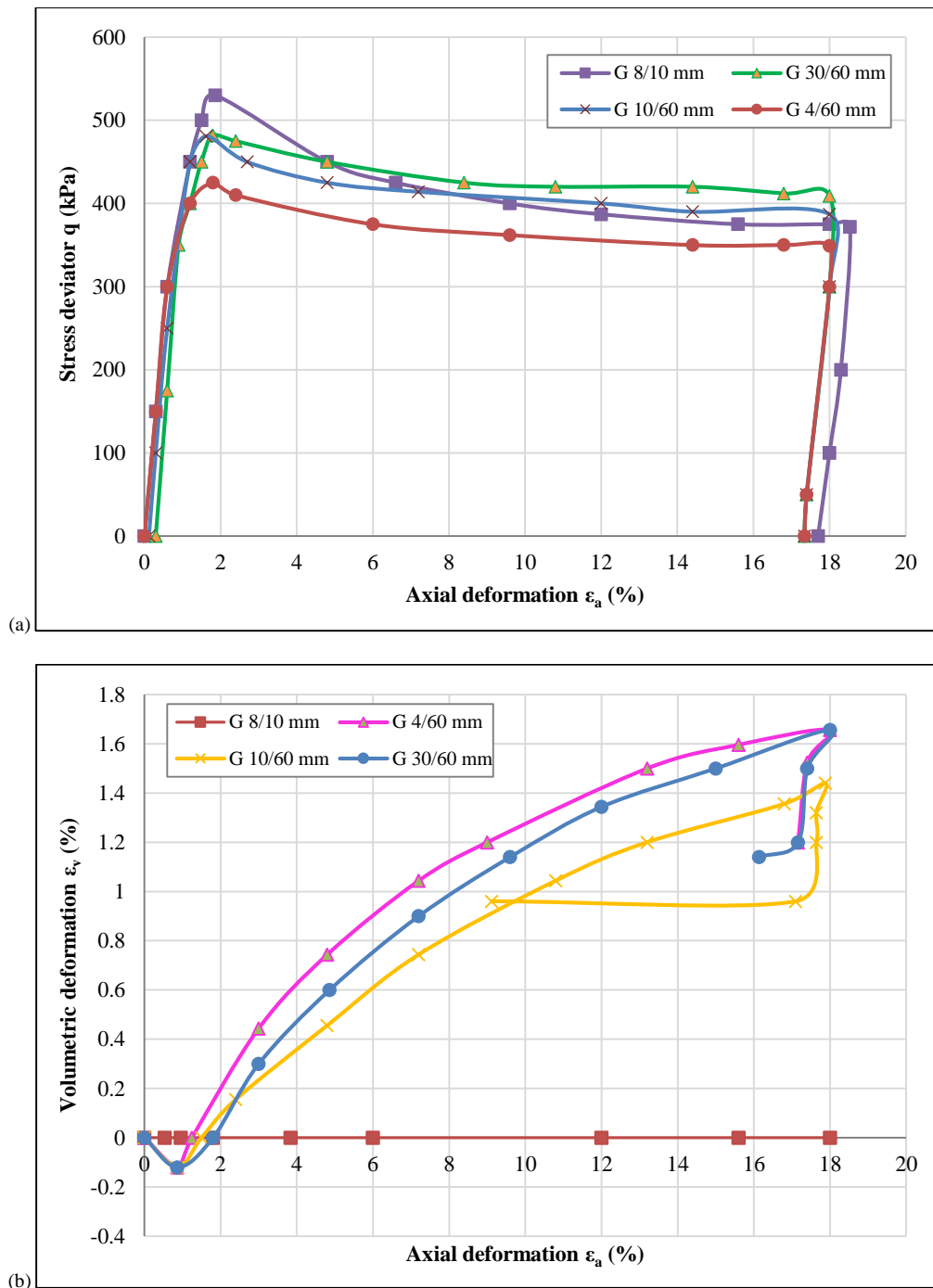


Figure 17. Influence of granulometric spread: (a) shear curves; (b) volumetric deformation curves ( $f_v=35\%$ ,  $I_D=0.8\%$  and  $\sigma'_c=100\text{kPa}$ )

For the two-volume fractions tested, it can be clearly seen that the tight mixture (in our case 8/10 mm), with  $f_v=35\%$ , has a greater maximum shear strength than the spread mixture (4/60 mm) and  $f_v=12\%$ . This is mainly due to the contact surfaces between gravels; which become more important when passing from a spread to a tight gradation [23, 24]. Thus, we notice that the soil with a spread gradation is less dilatant.

The same analysis performed on the 20% fraction of 4/60 mm and 30/60 mm gravels but with a loose matrix (Compactness Index  $I_D = 0.4\%$ ), similar results can be drawn from Figure 18.

## 5. Rupture Characteristics

Using Mohr Coulomb's criterion in the  $(\tau, \sigma')$  plane:  $\tau = \sigma' \tan \phi' + c'$ , the initial rupture characteristics of the tested soils are determined (Figure 19). Table 3 recapitulates the results obtained for all mixtures.

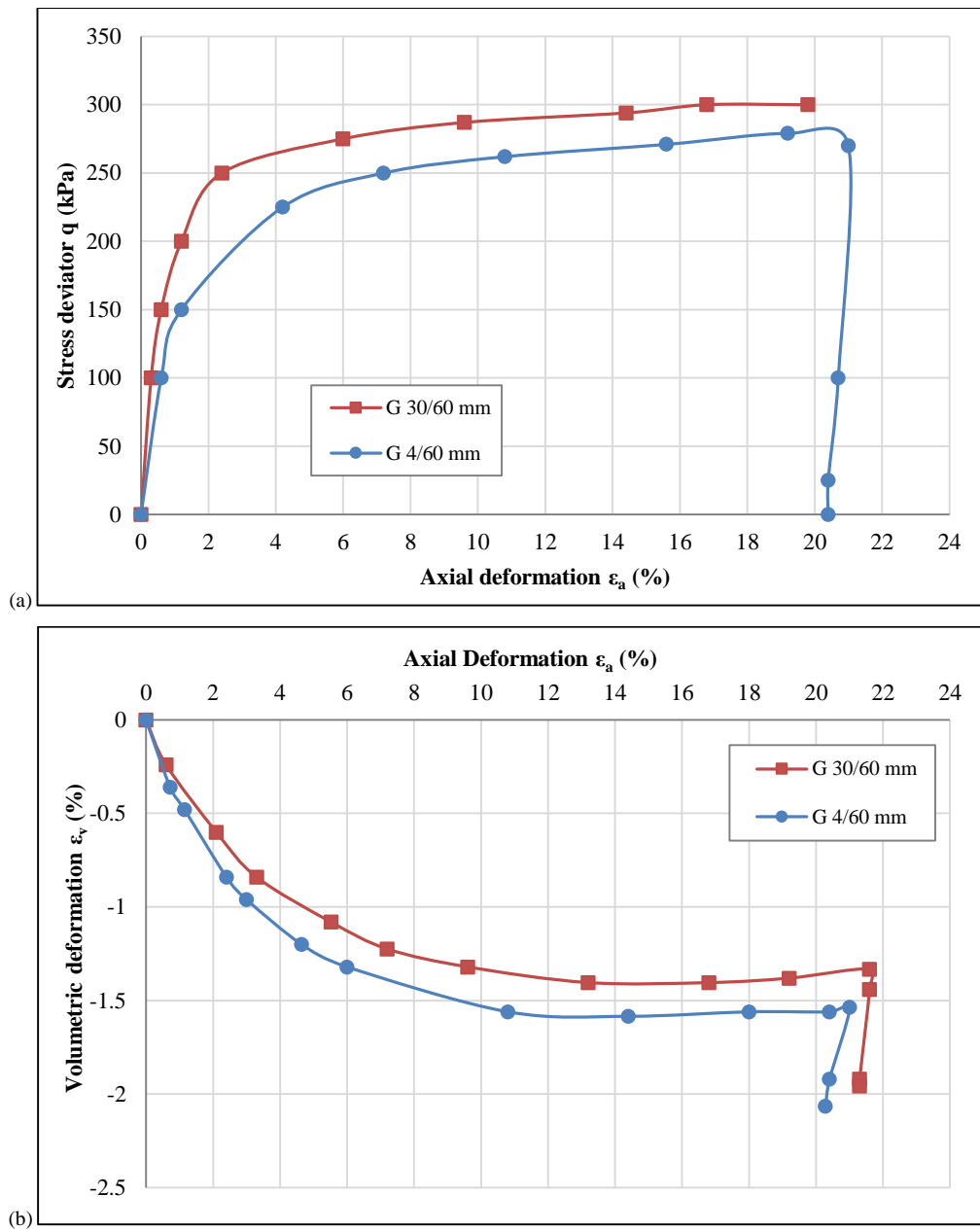


Figure 18. Influence of granulometric spread: (a) shear curves; (b) volumetric deformation curves ( $f_v=20\%$ ,  $I_D=0.4\%$  and  $\sigma'_c=100\text{kPa}$ )

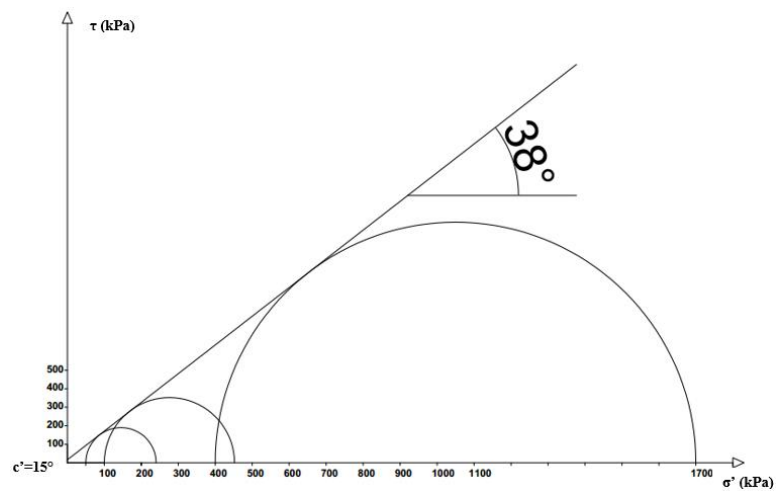
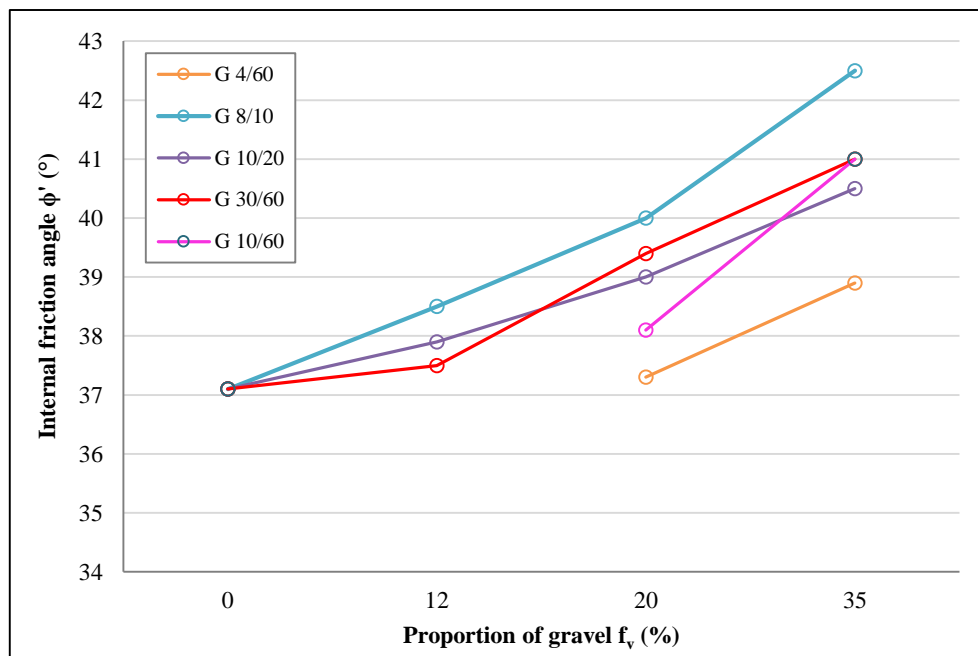


Figure 19. Rupture Mohr circles and intrinsic curve for a mixture with 10/20 mm inclusions and  $f_v = 20\%$

**Table 3. Cohesion and friction angle values for a mixture with 10/20 mm inclusions**

Gravel	$f_v$ (%)	0 %	12 %	20 %	35 %
G 8/10 mm	$C'$ (kPa)	10	8	12	15
	$\phi'$ (%)	37.1	38.5	40	42.5
G 10/20 mm	$C'$ (kPa)	8	10	15	10
	$\phi'$ (%)	37	37.9	38	40.5
G 30/60 mm	$C'$ (kPa)	8	9	11	8
	$\phi'$ (%)	37.1	37.5	39.4	41
G 10/60 mm	$C'$ (kPa)	16	-	10	10
	$\phi'$ (%)	37.1	-	38.1	41
G 4/60 mm	$C'$ (kPa)	20	-	15	15
	$\phi'$ (%)	37.1	-	37.3	38.9

In order to synthesize and better analyze the results of the table, curves showing the evolution of the angle of internal friction of the different soils as a function of the proportion of gravel have been drawn (Figure 20).

**Figure 20. Evolution of the internal friction angle  $\phi'$  as a function of the volume proportion of gravel**

The following conclusions are drawn:

- For all soils, the internal friction angle  $\phi'$  increases with increasing proportion of gravel.
- The increase is more pronounced in the case of uniform 8/10 mm gravel.
- For the same granulometric spread of the inclusions (10/20 mm and 30/60 mm), the values of  $\phi'$  are close, so the size of the inclusions does not have a significant influence on the value of  $\phi'$ .

## 6. Influence of the Compactness of the Matrix

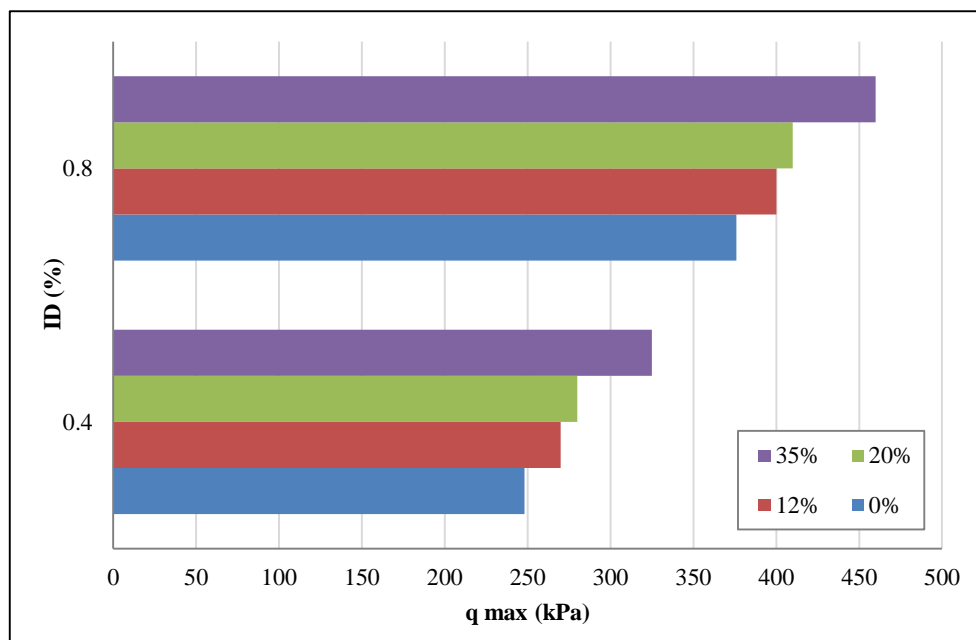
Regarding the effect of the void index of the sandy matrix, we conducted tests with two different states of compactness (loose, with  $I_D = 0.40$ , or dense, with  $I_D = 0.80$ ), and whose results have been reported in the previous paragraphs: It is noticed that, for all the soils, that the rupture strength of the dense soil corresponds to a marked peak. While in the loose case, the shear curve admits a horizontal asymptote corresponding to the maximum resistance  $q_{max}$ .

Here, the results of  $q_{max}$  as a function of  $I_D$  for the different types of gravel used and different volume proportion  $f_v$  (%) are grouped in Table 4.

**Table 4. Test characteristics showing the effect of sand density index  $I_D$  on the shear strength  $q_{max}$** 

Type of gravel	$f_v$ (%)	$\sigma'_c$ (kPa)	$I_D$ (%)	$q_{max}$ (kPa)	% of increase in $q_{max}$ as a function of $I_D$
G 30/60 mm	0	100	0.8	376	34.04
			0.4	248	
	20	100	0.8	425	31.76
			0.4	290	
G 4/60 mm	0	100	0.8	376	34.04
			0.4	248	
	20	100	0.8	380	27.63
			0.4	275	
G 10/20 mm	0	100	0.8	376	34.04
			0.4	248	
	12	100	0.8	400	32.50
			0.4	270	
	20	100	0.8	410	31.71
			0.4	280	
	35	100	0.8	460	29.35
			0.4	325	

It is clearly observed that the shear strength increases with the volume proportion of the inclusions in a similar way, and this independently of the compactness index  $I_D$  (Figure 21).

**Figure 21. The evolution of  $q_{max}$  from a loose state to a dense state as a function of the volume fraction of the gravel**

## 7. Conclusions

The study carried out with matrix coarse-grained soils, as a particular category of coarse soils, allowed us to better know and understand their geo-mechanical behavior from a parametric analysis, highlighting the effect of basic parameters on the mechanical characteristics, using the large-sized triaxial testing device. We studied the influence of the volume fraction  $f_v$ , the maximum diameter and the granulometric spread of the gravel, and the density index of the sand used. For the two states of sand compactness ( $I_D=0.4$  and  $I_D=0.8$ ), the results showed that:

- Soil shear strength increases with an increasing proportion of gravel. Therefore, the presence of inclusions within the matrix increases the strength of the soil. This result is compatible with the results obtained by the published literature.
- The increase is more marked in the case of 8/10 mm uniform gravel.

- For the same granulometric spread of the inclusions (10/20 mm and 30/60 mm), the resistance values are close, so the size of the inclusions does not have a significant influence on the  $q_{\max}$  value.
- The initial state of consolidation stress has no influence on the increase in shear strength in a dense state.
- Thus, we found that the shear strength is greater for a dense soil than for a loose soil.

It could be shown, in the final analysis, which the shear strength  $q_{\max}$  increases by about 32% when moving from a loose to a dense state.

It is necessary to underline the fact that the change of the sandy matrix by another clayey or silty one must be taken into account and be the object of research to be able the possibility of generalizing the results obtained in the case of the sandy matrix.

## 8. Declarations

### 8.1. Author Contributions

Conceptualization, G.A.; methodology, G.A., K.B., L.E., F.Z.L., and A.B.; validation, G.A., K.B., L.E., F.Z.L., and A.B.; formal analysis, G.A.; resources, K.B. and L.E.; data curation, G.A.; Investigation, G.A., K.B., L.E., F.Z.L., and A.B.; writing—original draft preparation, G.A.; writing—review and editing, G.A., K.B., L.E., F.Z.L., and A.B.; visualization, K.B., and A.B.; supervision, K.B. All authors have read and agreed to the published version of the manuscript.

### 8.2. Data Availability Statement

The data presented in this study are available in the article.

### 8.3. Funding

The authors received no financial support for the research, authorship, and/or publication of this article.

### 8.4. Conflicts of Interest

The authors declare no conflict of interest.

## 9. References

- [1] Kučová, E., & Kuvik, M. (2021). Evaluation of the mechanical properties of fluvial coarse-grained soils from dynamic penetration test. *IOP Conference Series: Materials Science and Engineering*, 1209(1), 012081. doi:10.1088/1757-899x/1209/1/012081.
- [2] Chang, W. J., & Phantachang, T. (2016). Effects of gravel content on shear resistance of gravelly soils. *Engineering Geology*, 207, 78–90. doi:10.1016/j.enggeo.2016.04.015.
- [3] Xun, X., Liang, H., & Xiaodong, H. Study on the relationship between energy evolution and strength parameters of coarse-grained soils in direct shear test. *Journal of Engineering Geology*, 29(5), 1331–1341. doi:10.13544/j.cnki.jeg.2020-522. (In Chinese).
- [4] Dorador, L. (2016). Experimental investigation of the effect of broken ore properties on secondary fragmentation during block caving. PhD Thesis, University of British Columbia, Vancouver, Canada. doi:10.14288/1.0319061.
- [5] Dorador, L. (2018). Density Estimation of Broken Materials in Sinkers Mining (Block/Panel Caving). 50<sup>th</sup> Chilean Geotechnical Congress, 3-5 December, 2018, Valparaíso, Chile. (In Spanish).
- [6] Stacho, J., & Sulovska, M. (2022). Shear Strength Properties of Coarse-Grained Soils Determined Using Large-Size Direct Shear Test. *Civil and Environmental Engineering*, 18(1), 244–257. doi:10.2478/cee-2022-0023.
- [7] Dorador, L. (2018). A Review of the Parallel Granulometry Methodology or Homothetic Curve Scaling applied to the Geotechnical Characterization of Coarse Grained Materials. 50<sup>th</sup> Chilean Geotechnical Congress, 3-5 December, 2018, Valparaíso, Chile. (In Spanish).
- [8] Dorador, L., Hoz, K., Salazar, F. (2018). Considerations in the geotechnical characterization of coarse grained materials. 50<sup>th</sup> Chilean Geotechnical Congress, 3-5 December, 2018, Valparaíso, Chile. (In Spanish).
- [9] Humire Guarachi, F. A. (2022). Liquefaction and Post-Liquefaction Behavior of Coarse-Grained Soils. Ph.D. Thesis, University of California, Davis, United States.
- [10] Dorador L., Poblete, M., Foretic, I. (2018). Minimum and Maximum Densities in Coarse-Grained Materials-Preliminary Results of an ongoing test program. 50<sup>th</sup> Chilean Geotechnical Congress, 3-5 December, Valparaíso, Chile. (In Spanish).
- [11] Dorador, L., & Urrutia, J. (2017). Geotechnical characterisation of coarse-grained soils containing weak and strong particles mixtures. 70<sup>th</sup> Canadian Geotechnical Conference (GeoOttawa 2017), 1-4 October, 2017, Ottawa, Canada.

- [12] Steger, S., Mair, V., Kofler, C., Pittore, M., Zebisch, M., & Schneiderbauer, S. (2021). Correlation does not imply geomorphic causation in data-driven landslide susceptibility modelling – Benefits of exploring landslide data collection effects. *Science of the Total Environment*, 776, 145935. doi:10.1016/j.scitotenv.2021.145935.
- [13] Ravindran, S., & Gratchev, I. (2022). Effect of Water Content on Apparent Cohesion of Soils from Landslide Sites. *Geotechnics*, 2(2), 385–394. doi:10.3390/geotechnics2020017.
- [14] Ardouz, G., Baba, K. (2020). Numerical Analysis of Instabilities Affecting an Excavation on the High Speed Line in Northern Morocco. *Advanced Numerical Methods in Foundation Engineering, GeoMEast 2019, Sustainable Civil Infrastructures*, Springer, Cham, Switzerland. doi:10.1007/978-3-030-34193-0\_9.
- [15] Ardouz, G., Baba, K., Ouadif, L. (2019). Modeling Landslides by the Finite Element Method: Application to an Embankment on a Railway in the Moroccan Rif. *Contemporary Issues in Soil Mechanics, GeoMEast 2018, Sustainable Civil Infrastructures*, Springer, Cham, Switzerland. doi:10.1007/978-3-030-01941-9\_11.
- [16] Ardouz, G., Baba, K., Bahi, L., & Cherradi, C. (2020). Comparison of analytical and numerical methods in the analysis of the stability of an excavation of the high-speed line in northern Morocco. 7<sup>th</sup> International Congress “Water, Waste and Environment” (EDE7-2019), E3S Web of Conferences 150, 1-7. doi:10.1051/e3sconf/202015003006.
- [17] Moulay Smaïne, G., Gueye, B., & Zoubir, B. (2014). Influence of grain size coarse soil on shear strength. *International Congress on Materials & Structural Stability, MATEC Web of Conferences*. doi:10.1051/mateconf/20141103009.
- [18] Honkanadavar, N. P., & Sharma, K. G. (2016). Modeling the triaxial behavior of riverbed and blasted quarried rock fill materials using hardening soil model. *Journal of Rock Mechanics and Geotechnical Engineering*, 8(3), 350–365. doi:10.1016/j.jrmge.2015.09.007.
- [19] Ovalle, C., Frossard, E., Dano, C., Hu, W., Maiolino, S., & Hicher, P. Y. (2014). The effect of size on the strength of coarse rock aggregates and large rock fill samples through experimental data. *Acta Mechanica*, 225(8), 2199–2216. doi:10.1007/s00707-014-1127-z.
- [20] Abozraig, M., Ok, B., & Yildiz, A. (2022). Determination of shear strength of coarse-grained soils based on their index properties: a comparison between different statistical approaches. *Arabian Journal of Geosciences*, 15(7), 1–17. doi:10.1007/s12517-022-09875-w.
- [21] Rashidi, M., & Rasouli, H. (2018). Initial hypotheses for modeling and numerical analysis of rock fill and earth dams and their effects on the results of the analysis. *Advances in Civil Engineering*, 2018. doi:10.1155/2018/3974675.
- [22] Sepehr, A., Hassanzadeh, M., & Rodriguez-Caballero, E. (2019). The protective role of cyanobacteria on soil stability in two Aridisols in northeastern Iran. *Geoderma Regional*, 16. doi:10.1016/j.geodrs.2018.e00201.
- [23] Wen, R., Tan, C., Wu, Y., & Wang, C. (2018). Grain size effect on the mechanical behavior of cohesionless coarse-grained soils with the discrete element method. *Advances in Civil Engineering*, 2018. doi:10.1155/2018/4608930.
- [24] Zhang, Z. L., Xu, W. J., Xia, W., & Zhang, H. Y. (2016). Large-scale in-situ test for mechanical characterization of soil-rock mixture used in an embankment dam. *International Journal of Rock Mechanics and Mining Sciences*, 86, 317–322. doi:10.1016/j.ijrmms.2015.04.001.